

## LETTERS

# Rapid heating of the atmosphere of an extrasolar planet

Gregory Laughlin<sup>1</sup>, Drake Deming<sup>2</sup>, Jonathan Langton<sup>1</sup>, Daniel Kasen<sup>1</sup>, Steve Vogt<sup>1</sup>, Paul Butler<sup>3</sup>, Eugenio Rivera<sup>1</sup> & Stefano Meschiari<sup>1</sup>

Near-infrared observations of more than a dozen ‘hot-Jupiter’ extrasolar planets have now been reported<sup>1–5</sup>. These planets display a wide diversity of properties, yet all are believed to have had their spin periods tidally spin-synchronized with their orbital periods, resulting in permanent star-facing hemispheres and surface flow patterns that are most likely in equilibrium. Planets in significantly eccentric orbits can enable direct measurements of global heating that are largely independent of the details of the hydrodynamic flow<sup>6</sup>. Here we report 8- $\mu\text{m}$  photometric observations of the planet HD 80606b during a 30-hour interval bracketing the periastron passage of its extremely eccentric 111.4-day orbit. As the planet received its strongest irradiation (828 times larger than the flux received at apastron) its maximum 8- $\mu\text{m}$  brightness temperature increased from  $\sim 800$  K to  $\sim 1,500$  K over a six-hour period. We also detected a secondary eclipse for the planet, which implies an orbital inclination of  $i \approx 90^\circ$ , fixes the planetary mass at four times the mass of Jupiter, and constrains the planet’s tidal luminosity. Our measurement of the global heating rate indicates that the radiative time constant at the planet’s 8- $\mu\text{m}$  photosphere is  $\sim 4.5$  h, in comparison with 3–5 days in Earth’s stratosphere<sup>7</sup>.

The giant planet orbiting the solar-type star HD 80606 is unique among the nearly 300 extrasolar planets that have been found so far<sup>8</sup>. On a three-month timescale, it shuttles between the inner edge of its parent star’s habitable zone and the highly irradiated close-in realm of the so-called hot Jupiters. Its extremely eccentric orbit provides compelling evidence of a peculiar dynamical history<sup>9</sup>, and the planet itself can be used as a laboratory to study the atmospheric dynamics of extrasolar planets. Clues to the planet’s interior structure can be gained by measuring the amount of tidal heating experienced by the planet. If its tidal quality factor,  $Q$ , is of order  $3 \times 10^5$  (consistent with that observed for Jupiter)<sup>10,11</sup> then tidal and stellar contributions to the planetary heating should be roughly equal, yielding an orbit-averaged effective temperature of  $T_{\text{int}} \approx 700$  K (ref. 9).

The solar-type parent star, HD 80606 (with  $M_\star \approx M_\odot$ ,  $R_\star \approx R_\odot$  and  $T_{\text{eff}} = 5,800$  K,  $M_\odot$  and  $R_\odot$  respectively being the solar mass and radius)<sup>8</sup>, has a binary companion, HD 80607, lying 17 arcsec to the east. Given the 58-pc distance to the system, this implies a projected separation of  $d \approx 1,000$  AU, and the two stars have nearly equal masses and luminosities. We monitored HD 80606 and HD 80607 continuously over a 29.75-h period using the 8- $\mu\text{m}$  channel of the NASA Spitzer Space Telescope’s<sup>12</sup> Infrared Array Camera (IRAC)<sup>13</sup>. We observed in stellar mode with a cadence of  $\sim 14$  s. Our observational campaign was timed to start  $\sim 20$  h before periastron. The geometry of the encounter is shown in Fig. 1. Before the observations, the planet’s orbital inclination was unknown, with the orbital geometry and stellar size indicating a  $\sim 15\%$  chance of occurrence of a secondary

eclipse centred on the epoch of superior conjunction ( $\sim 3$  h before periastron). Spitzer collected  $8,051 \times 256 \times 256$  pixel images during the observational campaign.

At periastron, HD 80606b responds to the pronounced increase in insolation by absorbing a fraction of the incident stellar radiative flux. A portion of this absorbed radiation is then re-radiated at 8  $\mu\text{m}$  in a time-varying manner. The rate of this emission depends on the detailed thermal, chemical and radiative properties of the atmosphere. At present, existing near-infrared observations of tidally circularized hot Jupiters present an incomplete and somewhat contradictory overall picture. It is not understood, for example, how the wind vectors and temperature distributions on the observed planets behave as a function of pressure depth, planetary longitude and planetary latitude. Most importantly, the effective radiative time constant in the atmospheres of short-period planets has not been directly measured, and as a result, dynamical calculations of the expected planet-wide flow patterns<sup>14–17</sup> have not come to a full consensus regarding how the surface flow should appear. The lack of agreement between the models stems in part from the paucity of unambiguous measurements of the basic thermal structure of the atmospheres of short-period planets. Hence, photometric near-infrared time series of planets such as HD 80606b that are subject to strongly time-dependent heating can provide crucial input data for the next generation of extrasolar-planetary global circulation models.

As expected from earlier experience with IRAC<sup>1,3,4</sup>, the data show the effect of a detector sensitivity that gradually increases with time. This rise (the ‘ramp’) amounts to several per cent over the course of our observations and is signal dependent, with strongly illuminated pixels showing a more rapid rise, followed by saturation. Removal of the ramp is complicated by image motion effects arising from tiny drift in the telescope pointing during the long-duration observation. The data contain a net  $\sim 0.5$ -pixel image motion over 30 h, encompassing both a long-term trend and a short-term (1-h) oscillation. Image motion affects the shape of the ramp for each pixel because the illumination of each pixel has a different time dependence and because the ramp has a logarithmic, rather than linear, shape. We therefore correct for the first-order (linear) shifting-of-photons effect simultaneously with a ramp correction based on a linear-plus-logarithmic term, as described in detail in the Supplementary Information. The comparison star was analysed using an identical method. An advantage of the per-pixel ramp removal is that it eliminates need to divide the HD 80606 time series by that of HD 80607, or to normalize with respect to it in any way. Instead, with ramp removal applied to both stars, the HD 80607 time series can be used as an independent control.

The calibrated time series for both HD 80606 and HD 80607 are shown in Fig. 2. Whereas the HD 80607 time series shows no

<sup>1</sup>UCO/Lick Observatory, University of California, Santa Cruz, California 95064, USA. <sup>2</sup>NASA/Goddard Space Flight Center, Planetary Systems Branch, Code 693, Greenbelt, Maryland 20771, USA. <sup>3</sup>Carnegie Institute of Washington, Department of Terrestrial Magnetism, 5241 Broad Branch Road, NW, Washington DC 20015, USA.

significant structure, there are several features of interest in the HD 80606 photometry. Most notably, there is an increase in flux of order  $\Delta F/F = 0.001 \pm 0.0002$  during the second half of the time series, which we interpret as arising from an increase in the planet's 8- $\mu\text{m}$  emission during the course of the observations.

We model the planetary response during the periastron encounter with a global, two-dimensional hydrodynamical model that employs a one-layer, two-frequency radiative transfer scheme<sup>17</sup>. We assume a planetary radius,  $R_{\text{pl}}$ , of 1.1 times that of Jupiter<sup>18</sup> and an  $i = 90^\circ$  orbit with the parameters given by the best-fit radial velocity solution, with the time of periastron adjusted to HJD 2454424.86. Given the planet's small periastron distance, it is expected that the planetary spin angular frequency,  $\Omega_{\text{spin}}$ , will have been pseudo-synchronized<sup>19</sup> to a rate that is similar to the instantaneous orbital angular frequency at periastron. There are several competing theories of the pseudo-synchronous frequency<sup>20</sup>. We adopt the following expression, where  $\Omega_{\text{orbit}}$  is the orbital angular frequency<sup>19</sup>:

$$\frac{\Omega_{\text{spin}}}{\Omega_{\text{orbit}}} = \frac{1 + (15/2)e^2 + (45/8)e^4 + (5/16)e^6}{(1 + 3e^2 + (3/8)e^4)(1 - e^2)^{3/2}} \quad (1)$$

This yields a planetary spin period of 40.7 h.

Our hydrodynamical model contains three free parameters. The first,  $p_{8\mu\text{m}}$ , is the atmospheric pressure at the 8- $\mu\text{m}$  photosphere; the second,  $X$ , corresponds to the fraction of the incoming optical flux that is absorbed at or above the 8- $\mu\text{m}$  photosphere; and the third,  $p_b$ , corresponds to the pressure at the base of our modelled layer. We adopt parameter values that put our model's light curve in good agreement with the observed high-signal-to-noise 8- $\mu\text{m}$  time series for HD 189733 (refs 4, 17). Specifically, we use  $p_{8\mu\text{m}} = 570$  mbar (adjusted for the surface gravity on HD 80606b, which is higher than that on HD 189733b),  $p_b = 4$  bar and  $X = 0.5$ . Our model photometric light curve is then obtained by integrating at each time step over the planetary hemisphere visible from Earth, and assuming that each patch of the planet radiates a black-body spectrum corresponding to the local temperature.

The photometry shows a noticeable dip of duration  $\sim 0.07$  d and amplitude  $\Delta F/F = 0.001 \pm 0.0002$  centred near HJD 2454424.74. We identify this feature with a secondary eclipse, as a result of two lines of evidence. First, our fit to the radial velocity data predicts a mid-secondary transit epoch of HJD 2454424.72  $\pm$  0.02, which is consistent with the centre of the observed feature. Second, we evaluate the significance of the detection using a bootstrap technique. From the full 8,051-frame time series, a sequence of 50,000 bootstrap trials is created on the basis of random scramblings of the deviations from our hydrodynamical model with no transit assumed. For each trial, we adopt a reverse top-hat function (of fixed predicted central transit duration of 0.07 d) and fit it to the data by varying the depth and time of the centre. We record the best-fit depth at each choice of time. For the real unscrambled data, the top-hat fit finds a maximum eclipse amplitude of 0.0015 near HJD 2454424.73. With the planetary and stellar properties given above, and with an  $i = 90^\circ$  orbit, the depth of the transit implies an 8- $\mu\text{m}$  brightness temperature for the planet of  $T_{\text{pl}} \approx 800$  K. The bootstrap trials indicate that this secondary eclipse has been detected with  $7\sigma$  confidence.

Having established the occurrence of the secondary eclipse, we can obtain a fit to the eclipse parameters. Using the flux baseline provided by the hydrodynamical model, we construct a grid of eclipse curves having different centre times, in-eclipse widths, and ingress/egress times. At each grid point, we fit the eclipse depth and the baseline with a scale factor using linear regression. The three-dimensional space of fitted parameters can be fully sampled, allowing for a direct determination of the minimum  $\chi^2$  value. Uncertainties are estimated using a standard bootstrap resampling procedure<sup>21</sup>. We find the following best-fit values: eclipse centre time,  $T_c = \text{HJD } 2454424.736 \pm 0.003$ ; ingress/egress times,  $T_{1,2} = T_{3,4} = 0.005 \pm 0.005$  d; in-eclipse time,  $T_{2,3} = 0.070 \pm 0.009$  d; eclipse depth,  $d = 0.00136 \pm 0.00018$ .

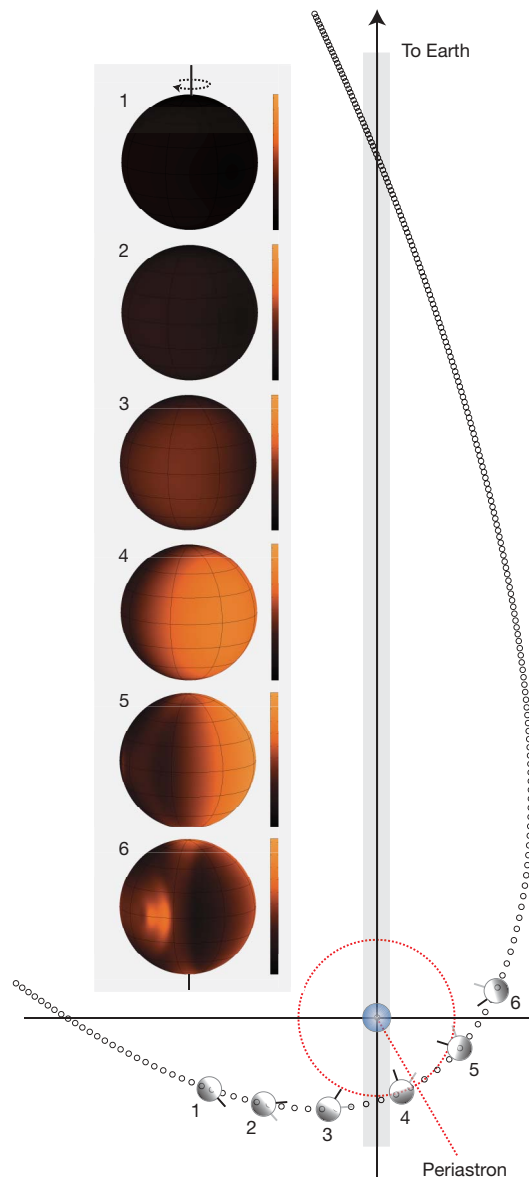


**Figure 1 | Orbital geometry of the HD 80606b system.** The small circles show the position of the planet in its orbit at 1-h intervals relative to the predicted periastron passage at HJD 2454424.84. The size of the parent star HD 80606 is drawn in correct relative scale to the orbit. The positions of the planet at times HJD (heliocentric Julian day) 2454424.2 (labelled 1), HJD 2454424.4 (2), HJD 2454424.6 (3), HJD 2454424.8 (4), HJD 2454425.0 (5) and HJD 2454425.2 (6) are shown, with the illuminated hemisphere indicated in each case. HD 80606b induces stellar reflex velocity variations of more than  $900 \text{ m s}^{-1}$ , and the stellar velocity can be measured to a precision of  $1.5\text{--}2.5 \text{ m s}^{-1}$  (ref. 25). This high reflex velocity signal-to-noise allows the planet's orbital parameters to be accurately determined, despite the relatively long orbital period. Using the Keck I telescope (W. M. Keck Observatory, Hawaii), we have extended our data set for HD 80606b to 62 Doppler velocities (tabulated in the Supplementary Information), which, when combined with previously published data<sup>7</sup>, give an orbital period of  $P = 111.4277 \pm 0.0032$  d, an eccentricity of  $e = 0.9327 \pm 0.0023$ , a longitude of periastron of  $\omega = 300.4977^\circ \pm 0.0045^\circ$ , and a radial-velocity half-amplitude of  $K = 471 \pm 5 \text{ m s}^{-1}$ . The accuracy to which the orbital elements can be determined enabled the scheduling of the Spitzer telescope to observe the star–planet system in the infrared during the periastron passage of 20 November 2007. The pseudo-synchronous rotation rate of the planet is indicated by the successive positions of the small black bar (located at the longitude containing the substellar point at periastron). The temperature distribution on the planet (as predicted by our hydrodynamical model, and as seen by an observer looking down the vertical axis) at times 1–6 is shown in the inset diagram. The temperature scale runs from 750 K (dark) to 1,800 K (light).

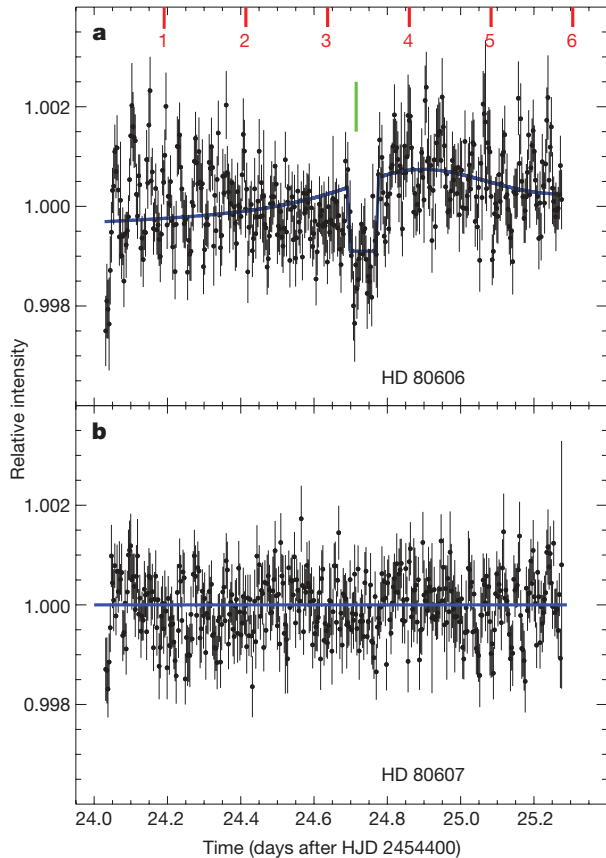


**Figure 2 | The light curve of a planet undergoing a close approach to a star.** Infrared photometric time series data for HD 80606 (a) and HD 80607 (b) for the Spitzer 8- $\mu\text{m}$  observations described in the text. The labels 1–6 correspond to the orbital positions indicated in Fig. 1. Our model light curve for HD 80606b is shown in blue, and the predicted midpoint for the secondary transit (from the fit to the radial velocities) is indicated in green. The model assumes an orbital inclination of  $i = 90^\circ$ . The depth and duration of the eclipse are determined by our estimates of the planetary and stellar sizes. The error bars on the photometric data indicate s.d., as described in detail in the Supplementary Information.

The secondary eclipse depth and our fit to the photometry indicate that HD 80606b had an effective temperature of  $T = 725\text{ K}$  at the beginning of the photometric observations, which is in accord with the energy output expected for tidal quality factors  $Q \geq 3 \times 10^5$ . Our model predicts that the planetary effective temperature on the Earth-facing hemisphere reaches  $T_{\text{max}} \approx 1,250\text{ K}$  before starting to decrease near the end of the observational window, and that the effective radiative time constant is  $\tau_{\text{rad}} = 4.5 \pm 2\text{ h}$  at the 8- $\mu\text{m}$  photosphere. The actual Spitzer 8- $\mu\text{m}$  photometry is broadly consistent with this model, although there is little indication of the predicted downturn at the end of the observations. If real, this apparent absence of a flux decrease could signal either rapid advection of heat onto the unilluminated hemisphere, or, alternatively, the failure of pseudo-synchronization theory to predict  $\Omega_{\text{spin}}$  correctly. The heating rate is consistent with predictions of detailed multi-frequency model calculations of ‘pL’-type cloud-free atmospheres<sup>22</sup>, and suggests that the optical albedo of the planet should be low, in agreement with optical full-phase photometry by the Canadian Microvariability and Oscillations of Stars satellite for hot Jupiters on tidally circularized orbits<sup>23</sup>.

The depth and duration of the secondary eclipse are consistent with an  $i \approx 90^\circ$  orbital inclination for HD 80606b, implying a probability of  $P \approx 15\%$  that the planet can also be observed in transit. Our radial velocity solution indicates that a central transit (were it to occur) would have a duration of 17 h, with a midpoint  $\sim 6\text{ d}$  after the secondary eclipse. Our predicted midpoint times are

$T_{\text{tr}} = \text{HJD } 2454653.68 + N \times 111.4277$ , where  $N$  is any integer. The long duration of the transit would allow for precise determination of parameters such as  $R_{\text{pl}}/R_\star$  and  $i$ . As a consequence of the planetary deceleration with respect to the star during the transit epoch, the resulting photometric light curve would harbour a detectable asymmetry. Transits would also enable unprecedentedly accurate spectroscopic measurement of the Rossiter–McLaughlin effect<sup>24,25</sup> giving the angle,  $\lambda$ , between the stellar rotational axis and the orbital angular momentum vector. If HD 80606b owes its current configuration to Kozai migration, then these two vectors would not be expected to be aligned.

Received 8 June; accepted 14 November 2008.

- Deming, D., Seager, S., Richardson, L. J. & Harrington, J. Infrared radiation from an extrasolar planet. *Nature* **434**, 740–743 (2005).
- Charbonneau, D. *et al.* Detection of thermal emission from an extrasolar planet. *Astrophys. J.* **626**, 523–529 (2005).
- Deming, D., Harrington, J., Seager, S. & Richardson, L. J. Strong infrared emission from the extrasolar planet HD 189733b. *Astrophys. J.* **644**, 560–564 (2006).
- Knutson, H. A. *et al.* A map of the day-night contrast of the extrasolar planet HD 189733b. *Nature* **447**, 183–186 (2007).
- Grillmair, C. J. *et al.* A Spitzer spectrum of the exoplanet HD 189733b. *Astrophys. J.* **658**, L115–L118 (2007).
- Langton, J. & Laughlin, G. Hydrodynamic simulations of unevenly irradiated Jovian planets. *Astrophys. J.* **674**, 1106–1116 (2007).
- Salby, M. L. *Fundamentals of Atmospheric Physics* 248 (Academic, 1996).
- Naef, D. *et al.* HD 80606b, a planet on an extremely elongated orbit. *Astron. Astrophys.* **375**, L27–L30 (2001).
- Wu, Y. & Murray, N. Planet migration and binary companions: The case of HD 80606b. *Astrophys. J.* **589**, 605–614 (2003).
- Goldreich, P. & Soter, S. Q in the solar system. *Icarus* **5**, 375–389 (1965).
- Peale, S. J. Origin and evolution of the natural satellites. *Annu. Rev. Astron. Astrophys.* **37**, 533–602 (1999).
- Werner, M. W. *et al.* The Spitzer Space Telescope mission. *Astrophys. J.* **154** (Suppl.), 1–9 (2004).
- Fazio, G. G. *et al.* The Infrared Array Camera (IRAC) for the Spitzer Space Telescope. *Astrophys. J.* **154** (Suppl.), 10–17 (2004).
- Cho, J. Y.-K., Menou, K., Hansen, B. M. S. & Seager, S. The changing face of the extrasolar giant planet HD 209458b. *Astrophys. J.* **587**, L117–L120 (2003).
- Burkert, A., Lin, D. N. C., Bodenheimer, P. H., Jones, C. A. & Yorke, H. W. On the surface heating of synchronously spinning short-period Jovian planets. *Astrophys. J.* **618**, 512–523 (2005).
- Showman, A. P., Cooper, C. S., Fortney, J. J. & Marley, M. S. Atmospheric circulation of hot Jupiters: Three-dimensional circulation models of HD 209458b and HD 189733b with simplified forcing. *Astrophys. J.* **618**, 559–576 (2008).
- Langton, J. & Laughlin, G. A new atmospheric model for HD 189733b. *Astrophys. J.* (submitted).
- Bodenheimer, P., Laughlin, G. & Lin, D. On the radii of extrasolar giant planets. *Astrophys. J.* **592**, 555–563 (2003).
- Hut, P. Tidal evolution in close binary systems. *Astron. Astrophys.* **99**, 126–140 (1981).
- Ivanov, P. B. & Papaloizou, J. C. B. Dynamic tides in rotating objects: orbital circularization of extrasolar planets for realistic planet models. *Mon. Not. R. Astron. Soc.* **376**, 682–704 (2007).
- Press, W. H., Teukolsky, S. A., Vetterling, W. T. & Flannery, B. P. *Numerical Recipes in FORTRAN. The Art of Scientific Computing* 2nd edn (Cambridge Univ. Press, 1992).
- Fortney, J. J., Lodders, K., Marley, M. S. & Freedman, R. S. A unified theory for the atmospheres of the hot and very hot Jupiters: Two classes of irradiated atmospheres. *Astrophys. J.* **678**, 1419–1435 (2008).
- Rowe, J. F. *et al.* The very low albedo of an extrasolar planet: MOST spacebased photometry of HD 209458. *Astrophys. J.* (submitted); preprint at (<http://arxiv.org/abs/0711.4111>) (2007).
- Queloz, D. *et al.* Detection of a spectroscopic transit by the planet orbiting the star HD 209458. *Astron. Astrophys.* **359**, L13–L17 (2000).
- Winn, J. *et al.* Measurement of spin-orbit alignment in an extrasolar planetary system. *Astrophys. J.* **631**, 1215–1226 (2000).

Supplementary Information is linked to the online version of the paper at [www.nature.com/nature](http://www.nature.com/nature).

**Acknowledgements** We thank P. Bodenheimer, D. Charbonneau, J. Fortney, N. Iro and H. Knutson for discussions. This work is based on observations made with the Spitzer Space Telescope, which is operated by the Jet Propulsion Laboratory (JPL), California Institute of Technology (Caltech), under contract to NASA. Support for this work was provided by NASA through an award issued by JPL/Caltech.

**Author Information** Reprints and permissions information is available at [www.nature.com/reprints](http://www.nature.com/reprints). Correspondence and requests for materials should be addressed to G.L. ([laughlin@ucolick.org](mailto:laughlin@ucolick.org)).